Fermi National Accelerator Laboratory

FERMILAB-FN-667

Background Reduction in the D0 Forward Muon Detector Using Thin Absorbers

D.S. Denisov, O.E. Krivosheev, N.V. Mokhov and V.I. Sirotenko

Fermi National Accelerator Laboratory
P.O. Box 500, Batavia, Illinois 60510

March 1998

Operated by Universities Research Association Inc. under Contract No. DE-AC02-76CH03000 with the United States Department of Energy

Background Reduction in the DØ Forward Muon Detector Using Thin Absorbers

D. S. Denisov, O. E. Krivosheev, N. V. Mokhov and V. I. Sirotenko

March 13, 1998

Fermi National Accelerator Laboratory
P.O. Box 500, Batavia, Illinois 60510

Abstract

Muon tracking detectors of both Fermilab collider detectors, DØ and CDF, typically have large number of background hits. The problem becomes severe in the Run II era. The studies show that background hits are mainly caused by soft electrons and indirectly by photons generated in hadron and electromagnetic showers and nuclear disintegration processes. With mean energy of electrons $\sim$1 MeV, there is a possibility to decrease number of correlated hits in detector layers consisting of separate planes by placing thin absorbers between the planes. Based on MARS and GCALOR simulations for polyethylene and aluminum absorbers, it is shown that a 3-mm aluminum sheet placed between the mini-drift tube planes in the DØ forward muon system provides a sevenfold reduction in the number of correlated hits. This reduces significantly fake muon trigger rate and muon track reconstruction inefficiencies, that makes the DØ forward muon system compatible with Run II requirements.

1 Introduction

Muon detectors at hadron colliders experience [1, 2] or will experience [3] the high occupancy due to background hits. Particles causing these hits are originated by showers induced mainly in the near-beam components both by products of pp ($p\overline{p}$) interactions at the interaction point (IP) and by beam loss in the vicinity of the detector [4]. Many of them are particles leaking through cracks in the detector elements and photons produced in thermal neutron captures and radionuclide decays. Introduction of local shielding and reduction of beam loss rates in the IP vicinity are the ways to mitigate the background problem [4, 5, 6, 7]. Although these methods

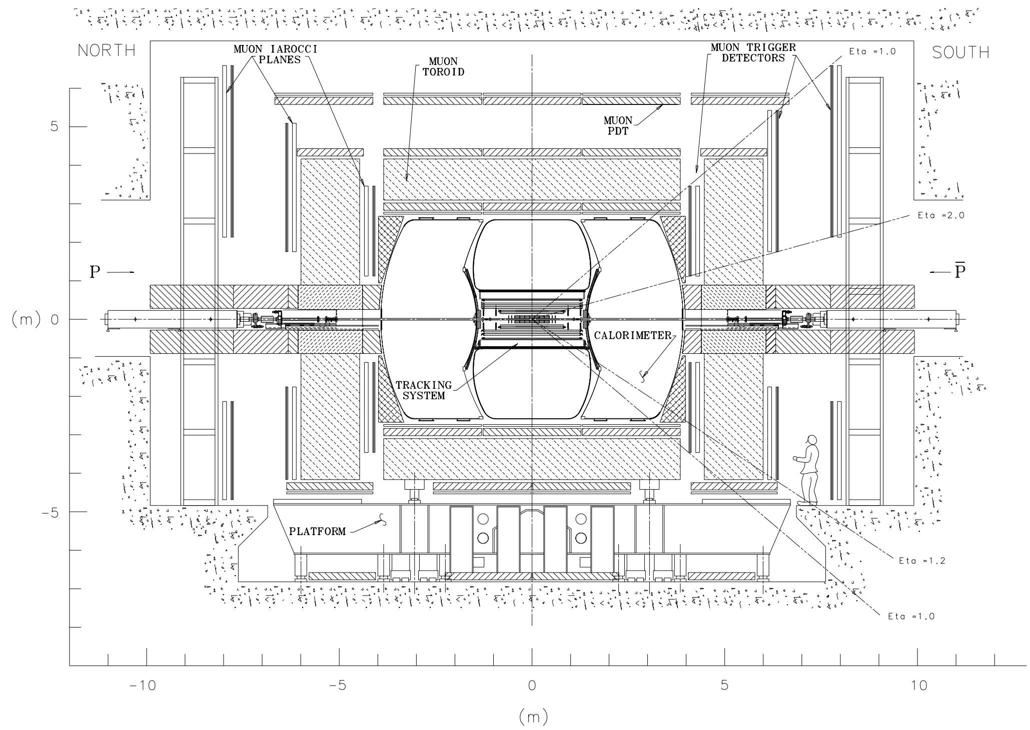

Figure 1: Side view of the DØ upgrade detector including various elements of the upgraded muon system.

can provide considerable reduction in background rates in detectors, they are usually expensive and require extra space in the detector. Fig. 1 shows the DØ detector upgrade with heavy shielding around the beam pipe to reduce backgrounds.

In this paper another way of background suppression is studied taking as an example a recently proposed DØ forward muon detector based on mini-drift tubes (MDT) [8]. Using realistic GCALOR and MARS13 calculations, it is shown that with a thin absorber between the MDT planes, correlated background rate can be significantly reduced: a 3-mm aluminum sheet reduces probability of fake track segment formation by a factor of $\sim$7. This will help in reduction of muon trigger rates as well as backgrounds in muon track reconstruction in the coming Run II at Tevatron.

2 MDT Based Muon Detector

In addition to the shielding, time and space correlations between hits is another way to distinguish between hits from IP-generated muons and background particles. This idea is exploited in a new design for the DØ forward muon tracking detector based on MDT. Detailed description of the proposed detector is given in [8]. As Fig. 2 shows, each A-, B- and C-layer of the DØ forward muon tracking detector [1] consists of four (nearest to the IP) or three MDT planes. Both GCALOR and MARS13 calculations show that with the proposed DØ shielding, the hits in the

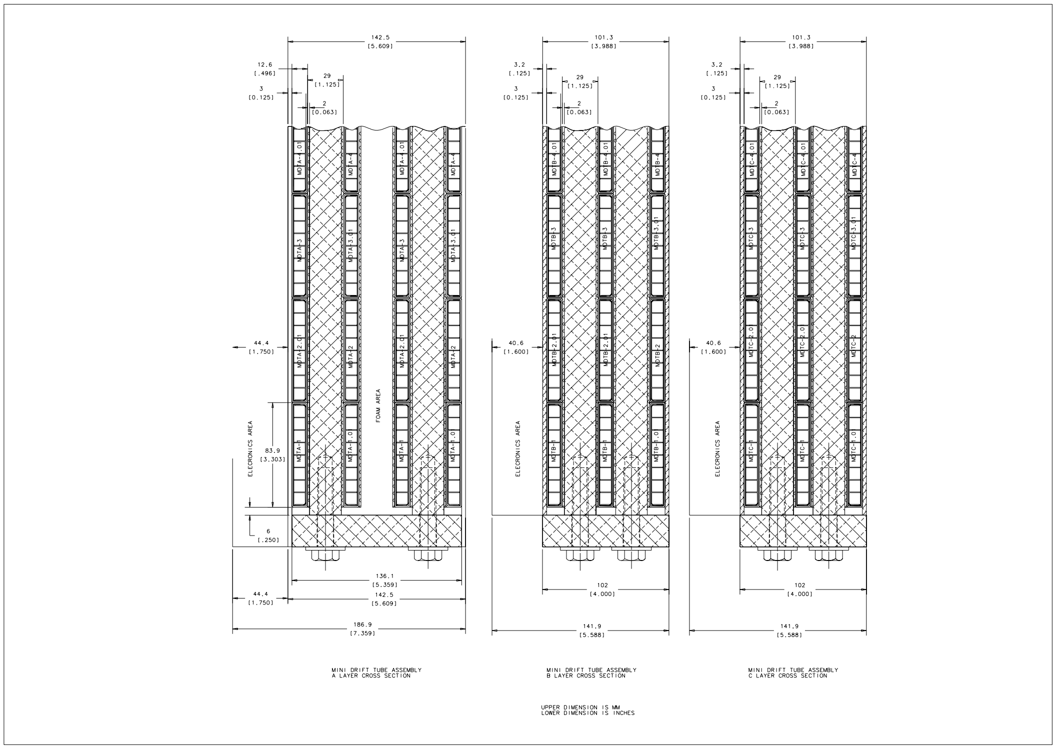

Figure 2: The layout of A-, B- and C-layers.

MDTs are mainly due to low-energy neutron interactions resulting in photon flux in the MDT/absorber bulk material. As a result, charged particle flux (and hits respectively) in the MDT sensitive volumes consists mainly of electrons with mean energy $\sim$1 MeV (see Fig. 4(a) below for an electron spectrum in MDT). Therefore, with a thin absorber between the MDT planes, the background electrons would not penetrate more than one detector plane. This way one prevents fake segment (local part of the track) formation by low energy electrons, while muons are easily detected.

3 Simulations

The effect of putting an absorber between two MDT planes have been estimated in two independent studies, performed using the GEANT-3.21 code with GCALOR interface [9], and the MARS13(97) code [10] linked to the Los Alamos code MCNP4A [11] for neutron and photon transport below 14 MeV. In both cases, the products of 1.8 TeV $p\bar{p}$ events generated with the DTUJET93 code [12] have been used. The cut-off energies were 1 MeV for charged hadrons and muons, 10^{-11} MeV for neutrons and 0.01 MeV for electrons and photons.

The upgrade geometry of the DØ detector was used (Fig. 1) with nominal shielding composed of 15-in iron and 6-in polyethylene followed by 2-in lead. Each MDT was described in this study as two boxes, with 1-mm poly walls (replaced at a later stage with 0.6-mm aluminum), filled with a gas (called here planes) separated by a 3-cm air gap. These MDT chambers were placed at their nominal positions in the DØ detector and all charged hits in the sensitive volumes of the MDT planes were recorded. Then, the number of hits was counted in each of the two MDT planes separately (*uncorrelated hits*). In addition, the number of *correlated hits* was counted, which were produced by the same charged particle in both planes. The following four MDT-absorber configurations have been studied:

1. Baseline – no absorbers, just air between two MDT planes.
2. 15-mm thick poly absorber between the planes.
3. 30-mm thick poly absorber between the planes.
4. Aluminum sheet 1 to 10 mm thick between the planes (MARS13 only).

3.1 GCALOR

The GCALOR calculated *x*-*y* hit distributions in a MDT plane are shown in Fig. 3 for the first, second, and both first and second planes for the configuration with a 15-mm poly absorber. Table 1 gives the number of *uncorrelated* and *correlated* hits for the first three MDT-absorber configurations averaged over all MDTs. As can be seen, there is practically no change in *uncorrelated* hit rate (in any particular single plane) versus putting an absorber between the planes. To the contrary, *correlated* hit rate depends strongly on the absorber presence. Reduction factors of ∼3 and ∼6 are obtained with a 15-mm and 30-mm poly absorbers, respectively.

Independent GCALOR calculations performed at the University of California at Davis by Yu. Fisyak and R. Breedon for the baseline and second (15 mm poly) configurations, gave also a small effect (∼10-20%) for *uncorrelated* hits, and 4.6, 4.9 and 3.6-fold reductions for *correlated* hits in the A-, B- and C-layers, respectively.

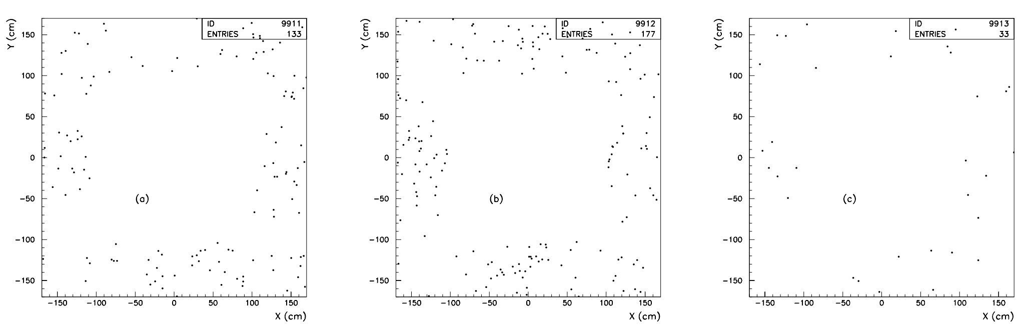

Figure 3: Hits in the MDT layers with a 15-mm poly absorber as calculated with GCALOR: (a) uncorrelated in the first plane; (b) uncorrelated in the second plane; (c) correlated for the both planes.

Table 1: Number of hits in the MDT planes as calculated with GCALOR.

Configuration	1	2	3
1st plane	186	133	164
2nd plane	189	177	230
Both planes	101	33	18

3.2 MARS13

MARS13 results are presented in Figs. 4 and 5. Fig. 4 shows that electrons in MDTs have low energy with mean of about 1 MeV, and that '*correlated*' electrons are peaked in the forward/backward directions.

Total *uncorrelated* charged particle flux (mainly electrons) in the first and second MDT planes of the B-layer, calculated with the MARS13 code, is presented in Table 2 for the MDT-absorber configurations 1 through 3 as a function of distance d (x or y) from the innermost MDT edge outwards. Results in the table are normalized per 10^7 source particles at MDT. One sees that effect of absorbers on single *uncorrelated* hits is less than 10 %.

Situation is different for *correlated* hits. Total *correlated* charged particle fluxes in the first and second MDT planes for the first three configurations are 2.3, 0.48 and 0.18 cm^{-2}, respectively, with the above normalization. Defining the absorber efficiency here as a ratio of charged particle flux in the MDT sensitive volume in the baseline configuration to that in the configuration with the absorber, one gets for the B-layer 4.8±0.7 with a 15 mm poly insertion and 12.8±3.2 with a 30 mm poly insertion. A good agreement between the GCALOR and MARS13 calculated absorber efficiency in the B-layer both for *uncorrelated* and *correlated* hits is encouraging.

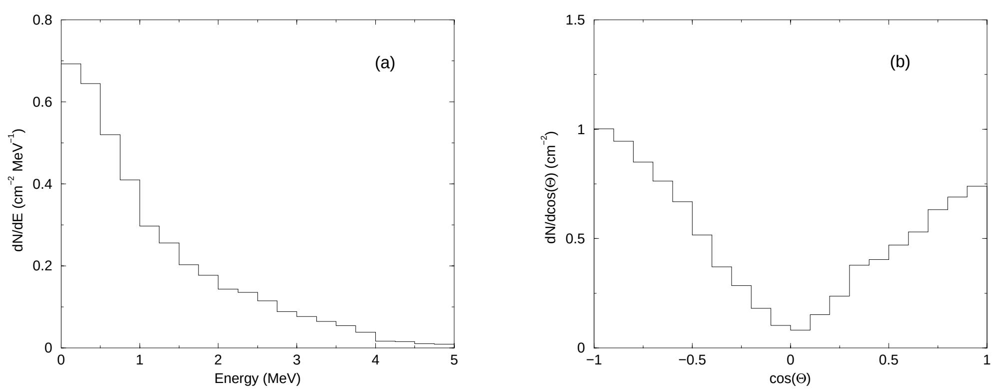

Figure 4: Typical electron energy spectrum (a) and angular distribution of correlated hits (b) in the MDT planes as calculated with MARS13.

Table 2: *Uncorrelated* total charged particle flux (cm^{-2}) in the first (p1) and second (p2) MDT planes for three absorber configurations. Typical errors are 10-15%.

Configuration	1	1	2	2	3	3
Plane	p1	p2	p1	p2	p1	p2
d (cm)						
0–25	8.0	8.3	10.1	7.1	8.9	9.9
25–50	8.6	8.9	9.0	8.8	11.0	12.7
50–75	9.9	9.1	11.1	9.7	10.0	7.5
75–100	8.3	8.4	9.6	7.7	8.1	8.8
100–125	1.5	2.1	2.2	2.3	1.1	1.2
125–150	0.15	0.26	0.27	0.14	0.18	0.11
Average	6.1	6.2	7.1	6.0	6.6	6.7

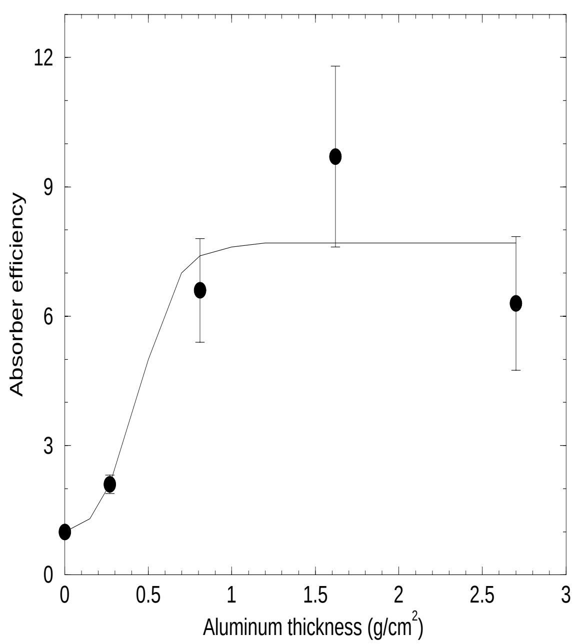

Figure 5: Efficiency of aluminum absorber between MDT planes *vs* its thickness calculated with MARS13.

Some spread in efficiency of the third configuration (30 mm poly) between GCALOR and MARS13 predictions, as well as between two independent GCALOR calculations, is most likely a reflection of low statistics in some Monte Carlo runs and slightly different shielding geometry, which is especially crucial for the C-layer. Calculated with MARS13 efficiency of the aluminum absorber between the MDT planes (B-layer) is presented in Fig. 5 as a function of the absorber thickness. As most background hits in MDT are produced by soft electrons, a rather thin aluminum sheet reduces drastically correlated hit rate in MDTs.

4 Conclusions

It has been demonstrated that a thin absorber between the MDT planes of the DØ forward muon detector provides significant reduction in the number of background correlated hits. Both poly and aluminum are good candidates for the insertions in the detector. Aluminum is a better choice for detector structural design. Reduction in fake track segment formation reaches its maximum of about seven at aluminum absorber thickness of 1 g/cm^2. A good agreement between GCALOR and MARS13 calculations for absorber efficiency both for *uncorrelated* and *correlated* hits gives a high degree of confidence in the Monte Carlo predictions.

References

[1] R. Jayanti et al., "The DØ Muon System Upgrade", Fermilab DØ Note-2780 (1996).

[2] "The CDF II Detector TDR", Fermilab-Pub-96/390-E (1996).

[3] CMS Technical Proposal, CERN/LHCC 94-38 (1994); ATLAS Technical Proposal, CERN/LHCC 94-43 (1994).

[4] N. V. Mokhov, Nuclear Physics B, **51A**, 210 (1996); A. I. Drozhdin, M. Huhtinen, and N. V. Mokhov, Nucl. Instruments and Methods in Physics Research, **A381**, 531 (1996).

[5] N. V. Mokhov, "DØ SAMUS Background Studies", Fermilab DØ Note-721 (1988) and Fermilab DØ Note-829 (1989).

[6] J. M. Butler, D. S. Denisov, H. T. Diehl, A. I. Drozhdin, N. V. Mokhov, and D. R. Wood, "Reduction of Tevatron and Main Ring Induced Backgrounds in the DØ Detector", Fermilab-FN-629 (1995).

[7] V. I. Sirotenko, "Shielding for DØ Detector: The First Look", Fermilab DØ Note-2512 (1995); N. V. Mokhov and V. I. Sirotenko, "Possible Minimal Solutions for DØ Detector Shielding Based on GCALOR and MARS13 Simulations", Fermilab DØ Note-2601 (1995); H. T. Diehl, "Aggressive Shielding Strategies for the Muon Upgrade", Fermilab DØ Note-2713 (1995); D. S. Denisov, H. T. Diehl, N. V. Mokhov, V. I. Sirotenko, and S. I. Striganov, "DØ Shielding Upgrade" (1996), unpublished.

[8] G. Alexeev et al., "Technical Design Report for the DØ Forward Muon Tracking Detector Based on Mini-drift Tubes", Fermilab DØ Note-3366 (1997).

[9] C. Zeitnitz, and T. A. Gabriel, Nucl. Instruments and Methods, **A349**, 106 (1994).

[10] N. V. Mokhov, “The MARS Code System User’s Guide, Version 13(95)”, Fermilab-FN-628 (1995); O. E. Krivosheev and N. V. Mokhov, “A New MARS and its Applications”, Fermilab-Conf-98/043 (1998); http://www-ap.fnal.gov/MARS.

[11] J. F. Briesmeister, editor, “MCNP - A General Monte Carlo N-Particle Transport Code”, Version 4A, Pub. LA–12625–M, LANL (1993).

[12] P. Aurenche, F. Bopp, R. Engel, D. Pertermann, J. Ranft, and S. Roesler, Comp. Phys. Com., **83**, 107 (1994).